The 4th International Conference
″Advanced Composite Materials Engineering ″
COMAT 2012
18- 20 October 2012, Brasov, Romania

NUMERICAL INVESTIGATION OF HEAT TRANSPORT PROCEDURE CAUSED BY HIGH POWERED UV LED

L. Kalmár [1], R. Hellmann [2], T. Régert [3], Z. Varga [4]
[1] University of Miskolc, Miskolc, HUNGARY, aramka@uni-miskolc.hu
[2] University of Applied Science, Aschaffenburg, GERMANY, Ralf.Hellmann@h-ab.de
[3] Senior Researcher, Karman Institute in Brussels, BELGIUM, tamas.regert@vki.ac.be
[4] University of Miskolc, Miskolc, HUNGARY, varga.zoltan.denes@gmail.com

Abstract: *In many industrial applications high powered UV light has a primary importance in the production process. Unfortunately the high power UV LED modules still generate a significant amount of heat energy that has to be efficiently dissipated in order to avoid the decrease of the output power and lifetime of the LED module. To realize the appropriate thermodynamic conditions for the UV LED modules, R&D efforts are being invested into the analysis of the physical processes inside the LED modules and their environment. The scientific part of the R&D project introduced in this paper consists of the simulation of the evolution of the temperature in the high power UV LED module taking into account the environment of the module and also the active air cooling.*

Keywords: *high powered UV LED modules, heat transport procedure, CFD simulation, air cooling system*

1. INTRODUCTION

High powered UV light radiation represents a significant component of several processes in several industrial applications. UV light is necessary in a very broad range of processes from drying, painting, food molecular treatment processes, biological and medical applications to fluorescent excitation based applications. Due to the nature of the generation of light by LED modules, the atomic transitions are accompanied by the generation of heat. The generated heat increases as the wavelength of the emitted light decreases. In other words, the emitted light energy in the UV range is only a small fraction of the invested energy through the alimentation. As the temperature of the UV LED module increases, the emitted light intensity decreases. Beside the decreased light intensity, the high temperature damages the material of the LED, too. Thus, to operate the LED modules correctly in the UV range, one must provide low temperature to obtain the ideal conditions for the generation of light.

The project introduced here is organized in the framework of an educational and scientific cooperation between two institutions: the University of Miskolc and the University of Applied Science, Aschaffenburg. The research is based on both experimental and numerical investigation of the thermodynamic transport processes in the 3x3 LED modules. The experimental research is carried out at the University of Applied Science, Aschaffenburg, while the numerical simulations are performed by the University of Miskolc. A description of the UV LED modules and their production is published in [1].

2. DESCRIPTION OF THE UV LED MODULE

The investigated LED module is represented in Fig. 1, where a substrate containing 9 LEDs was constructed. The 3x3 arrangement of the LED units allows us to assume symmetric conditions regarding the central unit that simplify the numerical modelling of the problem.

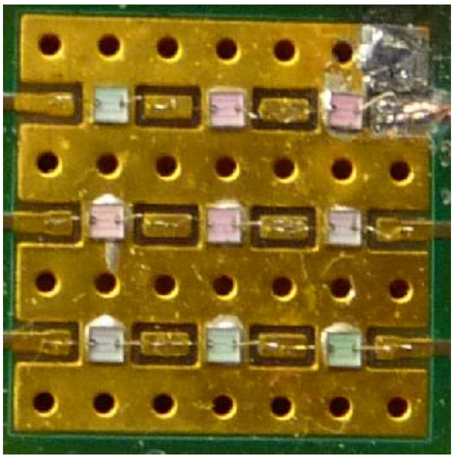

Figure 1: The investigated **3x3 LED module**

The LED units are small, light grey coloured, square-shaped elements in Fig. 1 that are mounted on a printed circuit board. A single LED unit can be observed in Fig. 2. The size of such a LED unit is 0.6 x 0.6 x 0.12 mm and its nominal power consumption is 390 mW. The electric conduction is realized on the usual way by a thin layer of copper (0.07 mm). However, in the present case, the copper layer serves also as a good heat conductor to guide away the significant amount of heat generated by the **3x3 LED module**s.

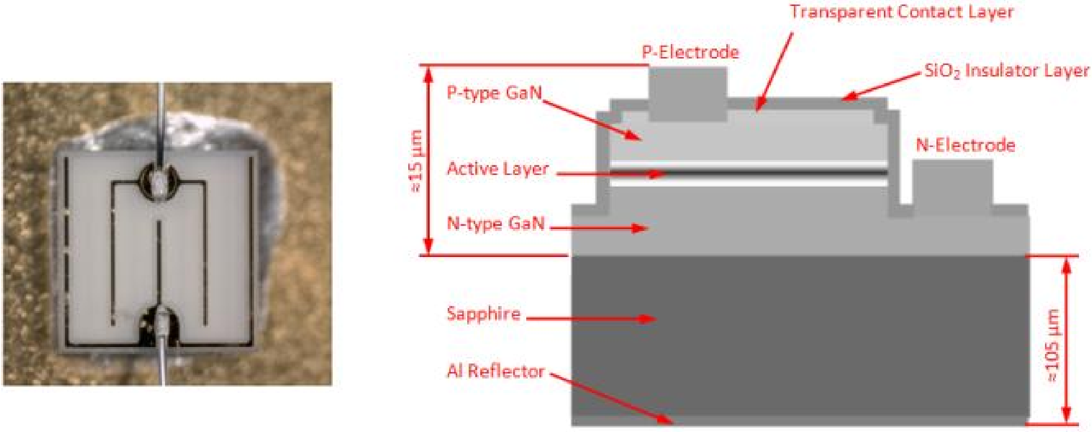

Figure 2: Photo and the schematic representation of the cross section of a single LED unit

The printed circuit board itself is a poor heat conductor, thus a solution had to be found to extract the heat from the copper plate. The developers of the UV LED substrate proposed the application of so-called “thermal via”-s, which are small pipes that are traversing the printed circuit board. The present substrate contains 7x4 thermal vias, that can be observed in Fig. 1 as circular holes in the copper layer. The drawing of the thermal vias can be seen in Fig. 3. In this figure also their cross section can be observed. The thermal vias are also made of copper and they are fixed to the thin copper layer on the top of the printed circuit board, that contains the LED module. The other end of the thermal via-s can be found on the other side of the printed circuit board. To make the cooling possible, this side of the printed circuit board is also coated by a thin layer of copper (0.07 mm thick). The heat generated on the LED module containing side of the board can thus be guided to its opposite side by traversing via the thermal vias. The side that does not contain the LED units can be cooled by the appropriate method.

The side of the printed circuit board that does not contain the LED modules was attached to a large aluminium frame (see Fig. 4) that increased the cooling surface and made it possible to mount a cooling fan onto it. The printed circuit board containing the LED module can be seen on the bottom of the upper image, represented by a small rectangle To improve the heat conduction between the contact surfaces of the copper layer and the aluminium frame, a silver paste was applied.

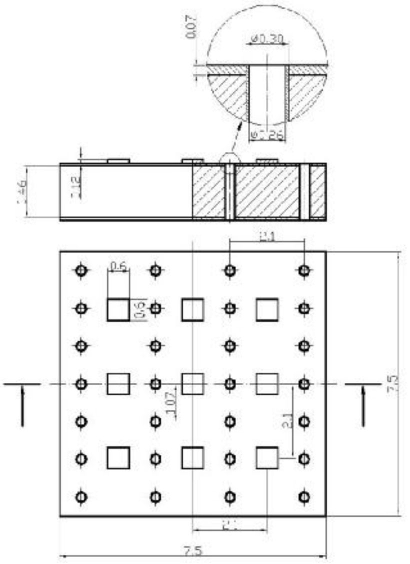

Figure 3: Drawing of the **3x3 LED module** showing also the thermal via-s

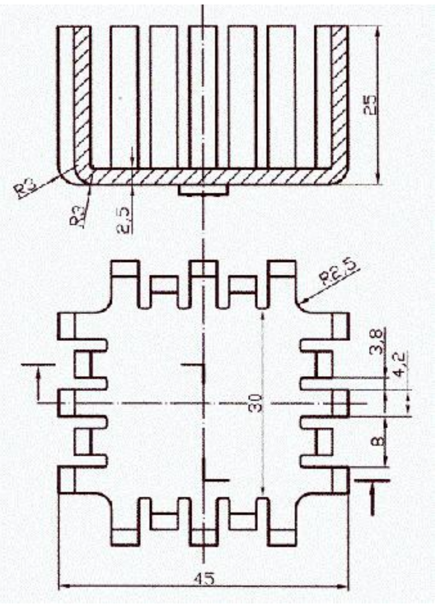

Figure 4: Drawing of the aluminium cooling frame

The cooling was realized by a fan of type **FD 6025** that was fixed to the ribs of the aluminium frame

3. COMPUTATIONAL MODEL OF THE UV LED MODULE

The partners of the cooperation R&D project decided to create a computational model that takes into account the 3D totality of the previously shown **3x3 LED module** attached to the aluminium frame. Due to the limitation of the computational resources some symmetry characteristics of the modelled device were exploited. The 3x3 matrix structure of the LED module made it possible to take only a quarter of the real device into account. The calculation model is noted by **M2** below. In this case the inhomogenity of the heating of the LEDs was neglected.

3.1. Geometry of the computational domain

The computational domain can be seen in Fig. 5. The domain contains the LED module noted by **M2**, the aluminium frame, and the cooling fan. The ribs of the aluminium frame are oriented upwards, thus the LED module is located on the bottom of the domain. The fan is modelled by a quarter of an annulus with an outer radius of 18 mm and inner radius of 8.5 mm, respectively. Although the cooling fan represents an outer surface of the domain, the aluminium frame is embedded and the external side surfaces represent the close outer vicinity of the whole device. This way it was possible to model the air flow past the ribs of the aluminium frame. In Fig. 5 the **3x3 LED module** is at the lower left corner of the upper image, attached to the bottom of the aluminium frame that is drawn by dashed line

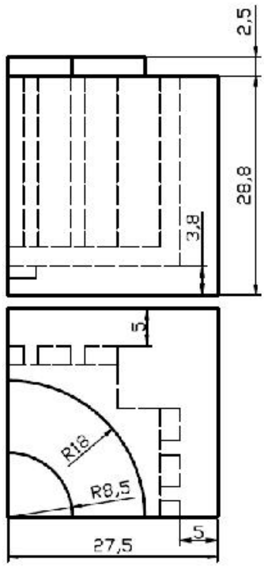

Figure 5: Computational domain **M2** for modelling the **3x3 LED module**

The quarter of the LED module is represented in Fig. 6. One can observe that the LED units are represented by square based bricks and their structural details were neglected. Also it can be seen that the copper layers both on the top and on the bottom of the module are contiguous. This latter simplification may be refined in the future because the gaps existing in the real model may influence the heat conduction in the plane of the copper layer.

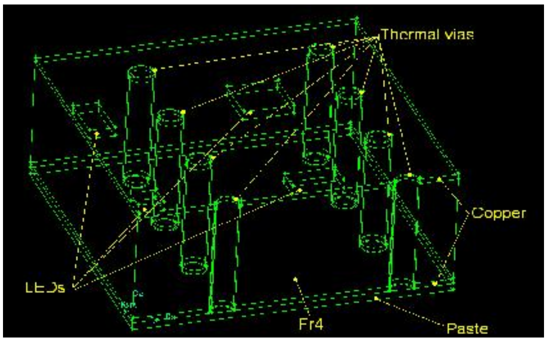

Figure 6: Model **M2**, the quarter of the **3x3 LED module**

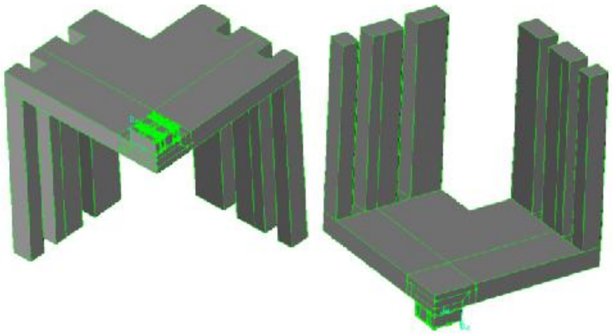

Figure 7: The **3x3 LED** module **M2** and the aluminium frame in two views

The heat conduction was computed in the volumes representing the copper layers and the thermal vias. The thermal characteristics of the copper and the **FR4** material of the printed circuit board were set in the FLUENT commercial software. The material of the LED was taken to be Sapphire, as this material makes up 88% of the LED unit. The copper had the following material properties: density 8920 kg/m3, heat capacity 385 J/kg K, thermal conductivity 400 W/m K. The printed circuit board material was characterized by: density 1800 kg/m3, heat capacity 385 J/kg K, thermal conductivity 0.4 W/m K. The aluminium frame had the following properties: density 2700 kg/m3, heat capacity 897 J/kg K, thermal conductivity 235 W/m K. The Sapphire that is the majority of the material of the LED units has: density 3980 kg/m3, heat capacity 25.2 J/kg K, thermal conductivity 25.2 W/m K.

The quarter of the aluminium frame with the LED module attached on it can be seen in Fig. 7. The aluminium frame was slightly simplified for easier meshing. It can be observed that the domain was characterized by regions of very different sizes. This character represents a difficulty in meshing and later computing the thermal and flow characteristics.

3.2. Meshing of the computational domain

The numerical solution of the governing equations of the given problem requires the volumetric discretization of the computational domain. The challenging feature of the present computational domain is the presence of a wide range of geometric features with orders of magnitude differences in the characteristic sizes.

The domain had mainly brick shaped topology that made it possible to generate a block-structured mesh almost everywhere. The overall mesh structure can be seen in Fig. 8. In regions where the mesh is not structured, the elements are still all hexahedral. In Fig. 8 the fan is on the bottom of the domain and the LED module is in the upper region where the grid points show a very high density.

The total number of hexahedral cells in the quarter domain was 2 067 563 cells. The grid quality is usually characterized by the skewness and the rate of change of the volume of the volume elements. In the present case the worst cell had an equi-angle skew below 0.8. The volume changes were fully controllable due to the mainly structured nature of the mesh. In the vicinity of the LED module the volume changes were kept below 1, while in the outer region where low velocities were assumed, a value of 3-4 was still accepted

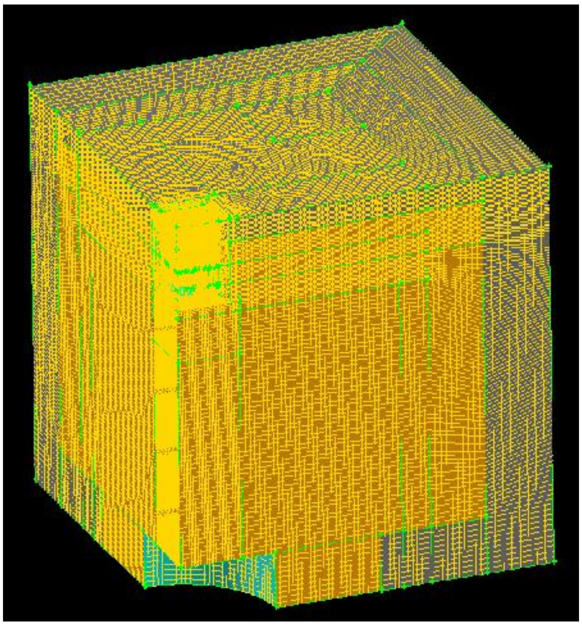

Figure 8: Mesh of the full domain **M2**

3.3. Boundary conditions

A coloured image in Fig. 9 indicates the different surfaces of the computational model on which various boundary conditions were imposed.

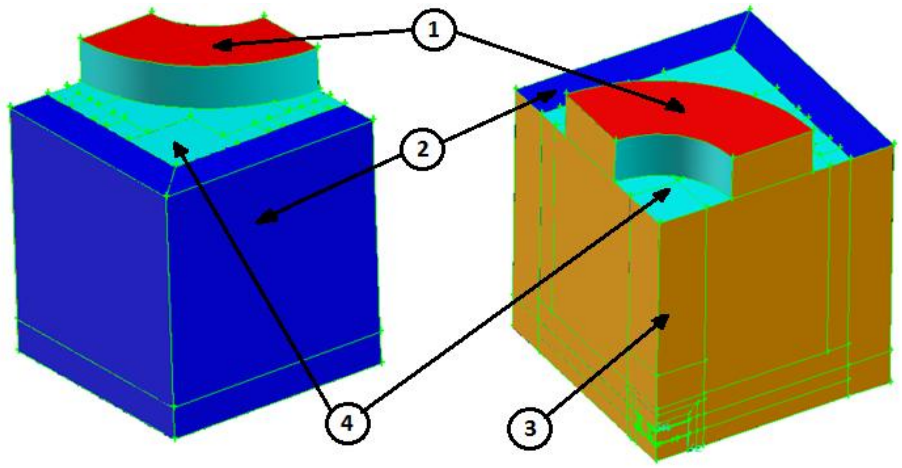

Figure 9: Boundary conditions of model **M2**

The surface of the active part of the fan is indicated by red and numbered 1. In the present configuration the fan was taken into account as if it had a fixed point of operation. Based on this assumption it was sufficient to prescribe the average mass flow across the surface. An advantageous feature of prescribing the average mass flow rate across a surface is that only the integral value and the direction of the incoming flow is fixed. The velocity distribution may vary. This feature is especially advantageous in the present case because the fan is situated very close to the cooled surface, so interaction between them is inevitable.

The outer surfaces of the domain that represent the connection with the free space are indicated by deep blue and numbered 2. On these surfaces constant pressure was prescribed. The air can traverse through these surfaces in an almost arbitrary direction (the direction is extrapolated from the interior of the computational domain), but can enter only in a wall-normal direction. Usually these surfaces should be far away from the modelled object, but in the present case the cell-number limitations required that they have a small distance.

The symmetry surfaces of the domain are indicated by brown and numbered 3. On these surfaces, by definition all surface-normal derivatives and the diffusion terms of all equations are set to zero. The symmetry surfaces thus act like a slip-wall, meaning that the flow cannot traverse across them, but there are no viscous effects either. From this aspect, the name “symmetry” is sometimes misleading, but it is the usual way of indication of this kind of boundary condition.

The no-slip wall boundary condition is indicated by cyan and numbered 4. Although in Fig. 9 only the upper wall surface is visible that surrounds the fan, it must be noted that this boundary condition was applied on all solid surfaces that had contact with the fluid. The wall boundary condition has the most important influence on the heat transfer properties between the fluid and the solid objects.

The LED units were modelled as volume heat sources and 360 mW power of heat was introduced into each of them. The introduced heat flow was treated as constant throughout the simulations and the temperature of the LEDs, as well as that of the other parts of the appliance, was obtained as a result of calculation

4. COMPUTATIONAL RESULTS FOR THE UV LED MODULE

To show the results it seems to be straightforward to analyse the problem by classifying it into two major groups: the characteristics of the solid objects and those of the fluid flow [2].

4.1. Heat transport procedure in solid objects

The solid objects of the computational domain are the LED module and the supporting aluminium frame. The computation was unsteady, thus the results are shown only for a given time instant (t=0.2 s after start-up). The temperature distribution in the vicinity of the LEDs is shown in the solid objects in Fig. 10. It can be observed that the top of the LEDs represent the hottest regions of the domain with a value of approximately 70°C. The heat is then transferred mainly into the upper copper layer. It can be seen that at this simulation the printed circuit board heats up in such a way that the temperature distribution along any of its horizontal sections is more or less constant. In these results the effects of the thermal vias are not visible. The temperature drops approximately 40°C across the printed circuit board and so the maximum temperature on the aluminium frame becomes 27°C.

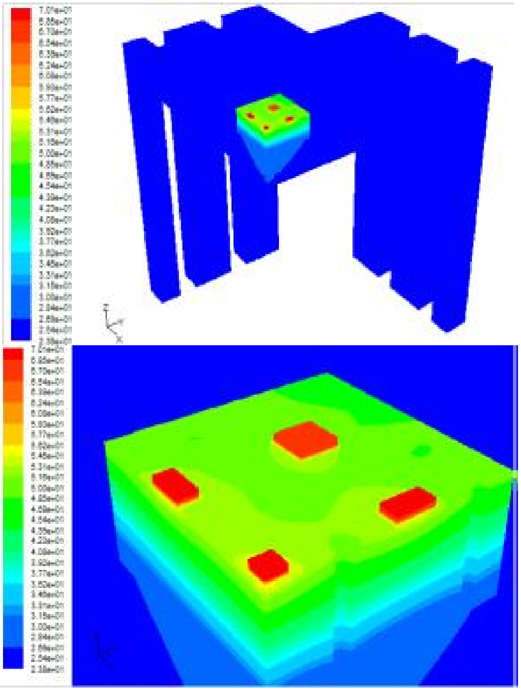

Figure 10: Temperature distribution at t= 0.2 s on the supporting aluminium frame and **3x3 UV LED module**

On the left image of Fig. 10 it can be seen how the heat is conducted from the LEDs into the aluminium frame. The overall temperature of the aluminium block is much lower than that of the LED module, thus the temperature distribution is not visible well on this scale

4.2. Heat transport procedure in fluid side

The major part of the computations is the determination of the flow field of the air that is cooling the solid objects. In the present model the main source of cooling was the fan, thus the LED module side of the domain was not treated especially on the fluid domain. In this representation the fan is blowing from the bottom to the top of the domain and the LED module is placed on the top. The temperature evolution on the top of the middle LED of the **3x3 LED module** is represented in Fig. 11.

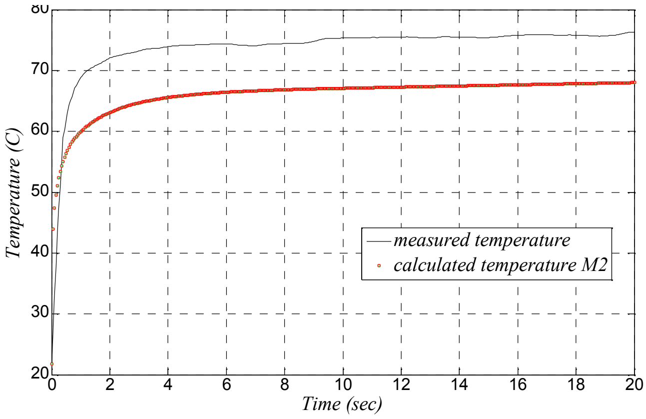

Figure 11: Temperature evolution in middle of the **3x3 UV LED module** over the LED unit there

5. CONCLUSION

The computational results showed good agreement with the experimental results concerning the rate of change of the temperature at the start-up transient of the LEDs. This indicates that the heat conduction model in FLUENT performs correctly. The material parameters seem to be well tuned

ACKNOWLEDGEMENTS

The work was carried out as part of the TÁMOP-4.2.1.B-10/2/KONV-2010-0001 project in the framework of the New Hungarian Development Plan. The realization of this project is supported by the European Union, co-financed by the European Social Fund.

REFERENCES

[1] Glaab, J.: Development of UV LED Modules for production technology and water purification, MSc. Thesis, University of Applied Science, Aschaffenburg, 2010.
[2] Varga, Z.: Numerical Simulation of Heat Transfer Procedure in High Power LED Modules, BSc. Thesis, University of Miskolc & University of Applied Science, Miskolc & Aschaffenburg, 2010.